Elevation dependence of drought legacy effects on vegetation greenness over the Tibetan Plateau

Peilin Li, Dan Zhu, Yilong Wang, Dan Liu

Elevation dependence of drought legacy effects on vegetation greenness over the Tibetan Plateau

Peilin Li[a], Dan Zhu[b,c*], Yilong Wang[d], Dan Liu[a]

[a] Key Laboratory of Alpine Ecology, Institute of Tibetan Plateau Research, Chinese Academy of Sciences, Beijing 100101, China.

[b] Institut de Ciència i Tecnologia Ambientals (ICTA), Universitat Autonoma de Barcelona, Barcelona, Spain.

[c] Laboratoire des Sciences du Climat et de l'Environnement, LSCE/IPSL, CEA-CNRS-UVSQ, Université Paris-Saclay, Gif sur Yvette 91191, France.

[d] Key Laboratory of Land Surface Pattern and Simulation, Institute of Geographical Sciences and Natural Resources Research, Chinese Academy of Sciences, Beijing 100101, China.

Corresponding author: Dan Zhu (zhudan.celia@gmail.com)

Abstract

Extreme drought events exert both immediate and prolonged influences on terrestrial ecosystems, yet the patterns and mechanisms of the delayed effects of extreme drought on alpine ecosystems remain largely unknown. In this study, we use satellite-derived normalized difference vegetation index (NDVI) data to examine the legacy effect of severe drought events on vegetation greenness across the Tibetan Plateau (TP). A pervasive, negative drought legacy effect, lasting about one year, is detected for all plant functional types including forests, shrubs and grasslands on the TP. The magnitude of the identified legacy effect, namely, the reduced growing-season NDVI in the first year post-drought, is spatially heterogeneous and exhibits a clear altitude dependence, while divergent relationships between elevation and the legacy effect are observed between alpine meadow and steppe. For alpine meadow, more pronounced legacy effects occur at higher altitudes with lower precipitation and temperature, suggesting a weaker drought resilience of alpine meadow under dryer and colder conditions. Whereas for alpine steppe, the magnitude of the negative legacies reduces as precipitation decreases along the elevation, which might be due to a greater adaptability to drought under more arid conditions that enables plant communities to recover to their normal state faster in these very dry regions. Our results advance the understanding of drought legacy effects on TP alpine ecosystems and highlight future avenues for research into how different alpine ecosystem types will respond to drought stress.

Keywords Vegetation greenness, Extreme drought, Legacy effect, Tibetan Plateau,

Alpine meadow, Alpine steppe.

1. Introduction

The frequency, intensity and duration of climate extremes have increased considerably during recent decades and are expected to increasingly impact future ecosystem dynamics and function (Dai, 2013; IPCC et al., 2013; Piao et al., 2019a). As one of the most frequently recurring climate extremes, drought could significantly reduce terrestrial ecosystem carbon sink via direct impacts such as water stress on vegetation growth (Ciais et al., 2005; Li et al., 2019b) and plant mortality caused by "hydraulic failure" or "carbon starvation" (Bréda et al., 2006; Mcdowell et al., 2008), as well as indirect impacts such as drought-induced increases in fires and pest and pathogen outbreaks (Allen et al., 2015; Brando et al., 2014; Piao et al., 2019b; Seidl et al., 2018). State-of-art earth system models have projected an increasing trend in the magnitude of annual vegetation productivity reductions associated with extreme droughts in the 21st century (Xu et al., 2019). However, global impact models tend to underestimate the negative effects of droughts on important sectors, including agriculture and terrestrial ecosystems (Schewe et al., 2019). One of the reasons for this underestimation might be the prevalence of incomplete and lagged vegetation growth recovery after severe droughts that are not well represented in ecosystem models (Anderegg et al., 2015b; Ogle et al., 2015; Reichmann et al., 2013). The effects of extreme drought on terrestrial ecosystems can last for several years and lead to reduced growth compared to normal years (Pederson et al., 2014), with

implications for carbon cycling. Therefore, an in-depth understanding and accurate simulation of this legacy effect is critical to our comprehension of the impacts of extreme drought events on ecosystem carbon cycles.

Legacy effects vary tremendously across biomes and plant functional types or even within species, which is likely linked to various ecophysiological traits and the interactive roles of bioclimatic status. In forest ecosystems, reduced tree growth after extreme drought events has been widely detected, based on both in situ tree-ring chronologies (Camarero et al., 2015; Liang et al., 2015; Pederson et al., 2014), and remote sensing data of vegetation greenness or primary productivity (Kannenberg et al., 2019b; Schwalm et al., 2017). Such negative legacy effects in forests can last from months to 1-4 years (Anderegg et al., 2015b; Huang et al., 2018), while longer legacy effects lasting up to 6 years have also been observed (Itter et al., 2019; Peltier et al., 2016). Whereas in grasslands and shrublands, drought legacy effects are less pronounced. Remotely sensed vegetation indices in northern temperate regions showed that shrubs and grasses experienced much shorter drought legacy effects than forests, with a maximum of one year for grasses (Wu et al., 2017). On the other hand, field measurements of aboveground net primary production (ANPP) in grasslands showed mixed results in terms of the magnitude and even direction of drought legacy effect. Sala et al. (2012) and Reichmann et al. (2013) found that the previous-year drought condition led to a less-than-normal ANPP for the current year, whereas Hoover et al. (2014) found a full recovery of ANPP in the first year after drought, and

65 Griffin-Nola et al. (2018) found even a positive drought legacy, i.e.
66 higher-than-normal ANPP in the year post-drought, in temperate grassland sites.

67 Mechanisms that may cause legacy effects within forest ecosystems have been
68 well discussed in recent studies. These mechanisms include leaf area and/or
69 non-structural carbohydrate loss, hydraulic damage (Anderegg et al., 2015b;
70 Anderegg et al., 2016), carbon allocation shifts, demographic traits such as species
71 composition shifts and mortality (Lloret et al., 2012), pest and pathogen outbreaks
72 (Anderegg et al., 2015a), and ecohydrological processes regarding water table
73 depletion and delayed replenishment (Kannenberg et al., 2019a; Kannenberg et al.,
74 2020). Some of these mechanisms, however, have a relatively lower impact on
75 grassland ecosystems, possibly explaining the more rapid recovery of grasses and
76 shrubs after droughts than forests (Jobbágy and Sala, 2000; Reichmann et al., 2013;
77 Sala et al., 2012).

78 Much of our current understanding of drought legacy effects comes from
79 tree-ring increments and forest inventories or syntheses relying on field measurements
80 in temperate grassland ecosystems (Anderegg et al., 2016; Gazol et al., 2017). Studies
81 of the lagged effects of drought on plant growth in arid and semi-arid alpine
82 ecosystems are however limited. A handful of such studies include field
83 measurements in alpine grasslands, which showed either a fast recovery of production
84 during the later re-wetting growing stage after the earlier summer drought (Chen et al.,
85 2020), or a delayed recovery of up to two years post-drought (De Boeck et al., 2018).

The Tibetan Plateau (TP), with a typical highland climate characterized by a low temperature, high solar radiation and limited water availability, plays an important role in shaping the regional and global climate and energy-water cycle (Duan and Wu, 2005; Huang et al., 2017a; Yao et al., 2019). With the harsh environment and complex terrain of the TP, alpine grassland is the dominant vegetation type, covering approximately two-thirds of the total plateau area, followed by shrubs that are mainly located in the central-southern region and forests along the southeastern boundaries where altitudes are relatively low (Cui and Graf, 2009) (Fig. 1). Rapid warming in recent decades over the TP has enhanced vegetation productivity by stimulating metabolism and extending growing season length (Huang et al., 2019; Piao et al., 2011; Piao et al., 2019c; Zhu et al., 2016). Nevertheless, warming can also exert negative impacts on plant growth on the TP due to drought conditions and warming-induced soil moisture loss (Fu et al., 2013; Zhang et al., 2015). Under such conditions, drought stress can regulate vegetation dynamics and mediate the effects of warming on vegetation on the TP (Li et al., 2020; Piao et al., 2014; Zhang et al., 2018). However, research on alpine ecosystems on the TP in response to extreme drought events and their legacy effects has been scant to date (Liu et al., 2019).

In light of current knowledge and gaps in the understanding of how extreme drought affects the TP terrestrial carbon cycle, we first tested whether extreme drought events in alpine ecosystems would lead to discernible legacy effects regarding greenness using the normalized difference vegetation index (NDVI). Second, we identified the duration, prevalence and magnitude of drought legacy effects as well as

their possible drivers, which is crucial for predicting the future behaviour of the alpine ecosystem and the provision of ecosystem services on the TP (Zhang et al., 2019b).

2. Materials and methods

2.1. NDVI dataset

The latest version of the Global Inventory Modeling and Mapping Studies (GIMMS) NDVI3g dataset derived from the Advanced Very High Resolution Radiometer (AVHRR) sensors (https://climatedataguide.ucar.edu/climate-data/ndvi-normalized-difference-vegetation-index-3rd-generation-nasagfsc-gimms) was used in this study. NDVI is an indicator of canopy greenness and has been commonly used for vegetation dynamic monitoring at regional and global scales (e.g. Barichivich et al., 2013; Huang et al., 2017b). GIMMS has the longest time series of NDVI observations that cover 1982–2015, with a spatial resolution of 0.083° and a biweekly temporal resolution (Jorge and Compton, 2014). The biweekly NDVI data were composited into monthly series using the maximum value composite (MVC) method. We defined the growing season as the period from May to September, and calculated growing-season average NDVI ($NDVI_{GS}$) that is used in the following analyses. Pixels with a multi-year mean $NDVI_{GS}$ value less than 0.1 during 1982–2015 were considered to be bare and sparsely vegetated areas and were excluded from the following analysis.

2.2. Climate data and drought variables

In this study, we use two drought variables to detect extreme drought events: climatic water deficit (CWD), defined as precipitation minus the potential evapotranspiration (PET) (Stephenson, 1998), and the standard precipitation-evapotranspiration index (SPEI), a climatic drought index based on a water balance that includes the effects of temperature variability on drought assessment that has the advantage of combining multiple scales (Beguería et al., 2014; Vicente-Serrano et al., 2010; Vicente-Serrano et al., 2013). We obtained two climate datasets to calculate these drought variables. One was the climate dataset for 86 meteorological stations with complete and continuous monthly meteorological records from 1982 to 2015 across the TP, collected from the China Meteorological Administration (CMA) (http://data.cma.cn/data/). Stations located at 3 × 3 pixels with an average $NDVI_{GS}$ less than 0.1 over the 34 years were excluded. As a result, meteorological data from 79 stations in the study area were processed, which were mainly located in the eastern, central and southern plateau. The other climate dataset was the gridded reanalysis forcing dataset at a 0.1° spatial resolution and 3 hour temporal resolution covering the same time period, obtained from the China Meteorological Forcing Dataset (CMFD), developed by the Data Assimilation and Modeling Center for Tibetan Plateau Multi-spheres, Institute of Tibetan Plateau Research, Chinese Academy of Sciences (http://data.tpdc.ac.cn/zh-hans/data/8028b944-daaa-4511-8769-965612652c49/?q=%E4%B8%AD%E5%9B%BD) (Chen et al., 2011; He et al., 2020; Yang et al., 2010).

For the CMA site-level dataset, we calculated monthly PET and SPEI (at a time-scale of 3 months) using the Food and Agriculture Organization of the United Nations (FAO-56) Penman-Monteith approach (Monteith, 1965) using the SPEI R package (Beguería et al., 2014; Vicente-Serrano et al., 2010). Driving inputs included latitude, elevation and monthly climate status, i.e., temperature, precipitation, wind speed, relative humidity and bright sunshine hours collected from meteorological stations. Note that bright sunshine hours were used to estimate solar radiation in this calculation. Then, monthly CWD was calculated as precipitation minus PET. Detailed calculation procedures are provided in http://spei.csic.es/home.html.

In terms of the gridded reanalysis CMFD, because solar radiation and daily maximum and minimum temperatures were not available, we calculated daily PET at a 0.1° resolution using the FAO-56 Penman-Monteith equation, with inputs including instantaneous near surface (2 m) air temperature, pressure, air specific humidity, wind speed and 3-hour mean surface downward shortwave and longwave radiation. Net radiation was calculated as the sum of downward components of shortwave and longwave radiation minus the sum of their upward components. The upward longwave was calculated using the surface air temperature (Blackbody radiation law). Upward shortwave was equal to downward shortwave multiplies albedo, following the method in (Sheffield et al., 2012). In this study, we used black-sky albedo in the visible band (ABD_BSA_VIS) as albedo data accessed from the Global Land Surface Satellite (GLASS) Product (Liang et al., 2013a; Liang et al., 2013b), downloaded from http://www.glass.umd.edu/. The ABD_BSA_VIS data had a geographic

resolution of 0.05°, and we aggregated to a 0.1° resolution prior to the calculation to match the CMFD data resolution. Through the above procedures, daily PET data were converted to monthly accumulative PET, and then, monthly CWD was obtained by subtracting PET from precipitation. Accordingly, monthly precipitation and PET were determined to calculate the SPEI using the R package. Finally, we resampled the gridded monthly CWD and SPEI data to a resolution of 0.083° to match the spatial resolution of NDVI. The growing season CWD and SPEI were produced by averaging the corresponding values from May to September.

2.3. Land cover and digital elevation model (DEM) datasets

The land cover map of TP was extracted from the 1:1000,000 digitalized vegetation map of China (Editorial Board of Vegetation Map of China, 2001, http://westdc.westgis.ac.cn), and it was mapped in Figure 1 and in our previous study (Li et al., 2020). The elevation data were obtained from the Advanced Spaceborne Thermal Emission and Reflection Radiometer Global Digital Elevation Model version 2 (http://earthexplorer.usgs.gov/), with a spatial resolution of 30 m. We aggregated the elevation data into a 0.083° resolution using the bilinear interpolation method. To obtain an overall view of vegetation greenness across the plateau, we drew the contour lines of the multi-year mean $NDVI_{GS}$ during 1982–2015. The topography and vegetation types of the TP and the contour map of the mean $NDVI_{GS}$ are shown in Figure 1, showing a decrease in $NDVI_{GS}$ from the southeastern forest region to the western desert region along an increasing altitude gradient.

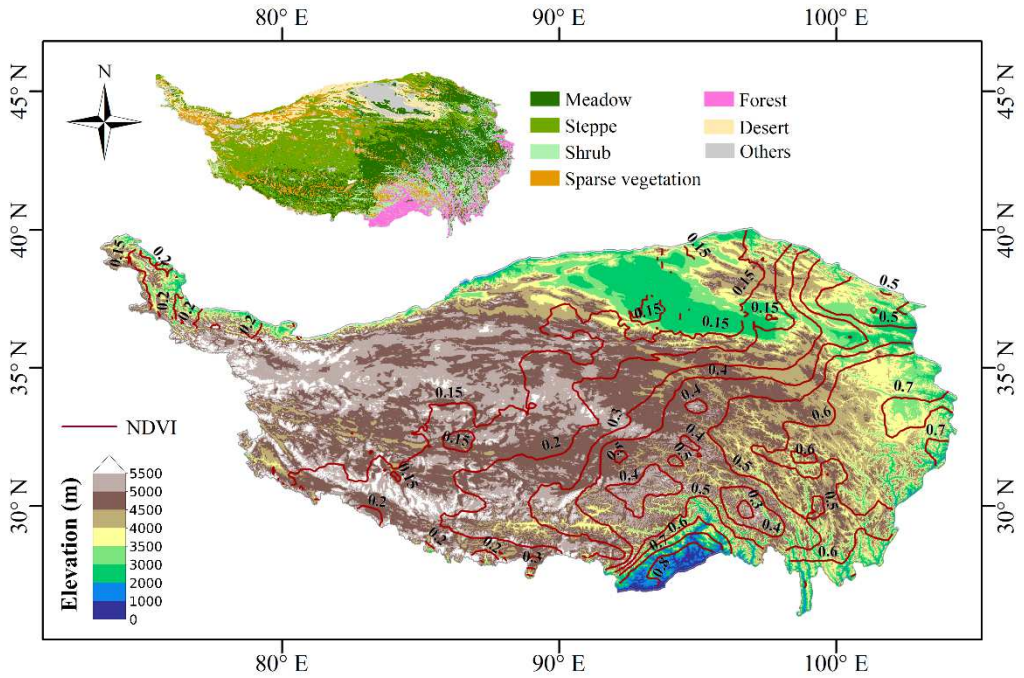

Fig. 1. The topography (m, above sea level) of the Tibetan Plateau (TP) and the isolines of multi-year average growing season (May-September) NDVI during 1982–2015 over the plateau. Inset shows the vegetation types across the TP.

2.4. Drought legacy on vegetation greenness

In this study, we identified extreme drought events as the years with detrended growing season drought variables (i.e., CWD and SPEI) exceeding 1.5 standard deviations (1.5-SD dry anomaly). To avoid consecutive drought events disturbing the following year plant recovery, only single drought events lasting no more than one year and no consecutive drought in the following 3 years were considered. The legacy effect in growing-season vegetation greenness, i.e., $NDVI_{GS}$, was quantified using two methods: (a) partial autocorrelation function (PACF) coefficients of yearly $NDVI_{GS}$, and (b) the departure of observed $NDVI_{GS}$ from predicted $NDVI_{GS}$ after extreme

drought events based on long-term correlations between growing season NDVI and drought variables. PACF identifies the extent of the lag in a time series (i.e., yearly $NDVI_{GS}$ in this study) while conditioning on the values at all smaller lags (Ramsey, 1974). It is a simple and widely used way to measure legacy effects in time series (Scheffer et al., 2009).

The second method generates a prediction of post-drought greenness after each extreme drought event, calculated by linear regressions between drought variables and $NDVI_{GS}$ over the period of 1982−2015, as in previous studies (Anderegg et al., 2015b; Huang et al., 2018; Sala et al., 2012). In this method, the reliability of the drought legacy depends on the strength of the correlations between the growing season NDVI and drought variables. Time series of $NDVI_{GS}$ and two drought variables were detrended and normalized prior to linear regressions. The legacy effect at each pixel or station was determined by averaging the departure values between the observed and predicted $NDVI_{GS}$ after all extreme drought events. Following the same procedures, we also calculated legacy effects using residuals of $NDVI_{GS}$ from which the effects of temperature were removed by linear regression. Finally, pixels or stations central at 3×3 pixels with a multi-year average $NDVI_{GS}$ smaller than 0.1 over the 34 years were excluded from the analysis. To investigate the altitude gradient of drought legacy effects on $NDVI_{GS}$, we calculated the mean legacy effect in each elevation bin at an interval of 100 m. When calculating legacy effects in elevation bins, only the pixels with significant and positive correlations between NDVI and drought variables were included.

3. Results

3.1. Drought legacy effects on vegetation greenness of alpine grass, shrubs and forests

We detected prevalent drought legacy effects on vegetation greenness that lasted for one year across the TP, i.e., reduced growth in the first year after drought and expected growth recovery in the second year. Positive PACF coefficients deduced from SPEI, which indicated detectable legacy effect of $NDVI_{GS}$, were observed in more than 80% of all pixels and in approximately 91% of the pixels with significantly positive NDVI-SPEI relationships in the first year after extreme drought. Such widespread positive PACF coefficients occurred regardless of the vegetation type (Fig. 2). The results derived from the CWD were similar to those derived from SPEI and are thus not shown here. One-year drought legacy effects in grass, shrub and forest were also observed based on the linear regression method (Fig. 3). In addition, drought legacy effects lasting for 1 year were robust regardless of the strength of the correlation between drought stress and $NDVI_{GS}$ (Fig. A1). For both results derived from all grid points and meteorological sites, $NDVI_{GS}$ had comparable magnitudes of negative legacy effects: approximately 0.33 times the SD decrease in observed versus predicted $NDVI_{GS}$ in the first year post-drought. However, grids/sites with significant and positive NDVI-SPEI relationships exhibited larger negative legacy effects than those derived from all grids/sites (Fig. 3). Furthermore, negative legacy effects tended to be larger where the interannual variability in $NDVI_{GS}$ was more strongly correlated with water limitation (Fig. A1).

Slight differences were found regarding the magnitude of drought legacy effects among different plant functional groups (PFGs). In the first year after severe drought, the magnitude of the negative legacy effects deduced from the SPEI was largest on shrubs, followed by that on forests, alpine meadows and steppes (Fig. 3). This phenomenon was relatively more evident in pixels with a significantly positive correlation between $NDVI_{GS}$ and water availability. Reductions in the normalized $NDVI_{GS}$ (observed minus predicted) of shrub (0.51) were ~1.2 times more pronounced to those of alpine meadow (0.43) and ~1.5 times to those of alpine steppe (0.33) in pixels where the $NDVI_{GS}$ exhibited significant correlations with SPEI (Fig. 3). The results from the CWD showed overall comparable magnitudes of legacy effects between different PFGs and generally larger negative legacy effects compared with those derived from SPEI, especially in the pixels/sites in which $NDVI_{GS}$ was significantly correlated with drought stress (Fig. A1). Moreover, there was no significant correlation between the magnitude of the legacy effect and the intensity of the corresponding drought event ($p > 0.1$, Fig. A2), indicating that the magnitude of the legacy effects was unlikely attributable to differences in drought severity.

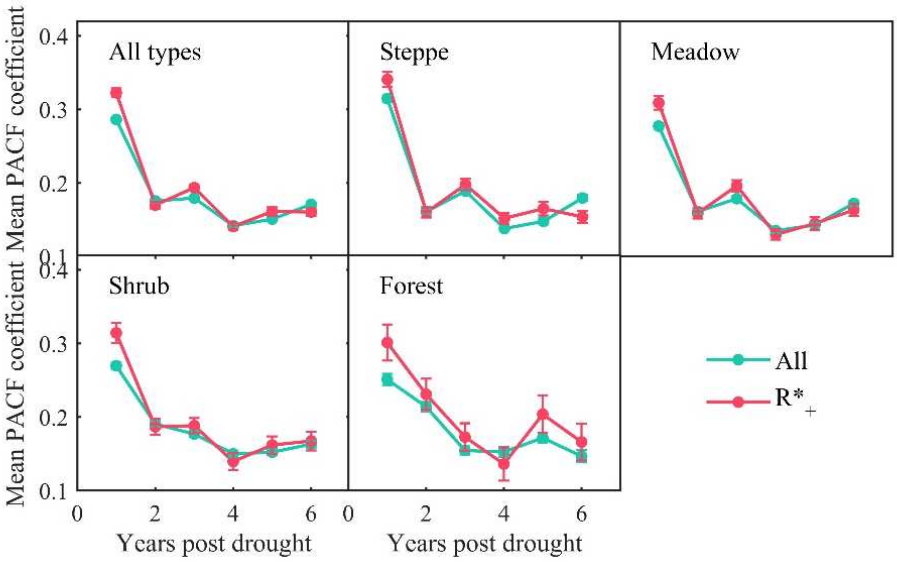

Fig. 2. Legacy effects detected based on partial autocorrelation function (PACF) coefficients of growing season NDVI. The mean PACF coefficients across pixels with positive PACF coefficients in the corresponding year are shown here. Turquoise line represents mean value of all pixels (All) and pink line represents the pixels where NDVI is significantly positively correlated with SPEI (R^*_+). Error bars represent 95% confidence intervals around the mean from 1,000 bootstrapped estimates.

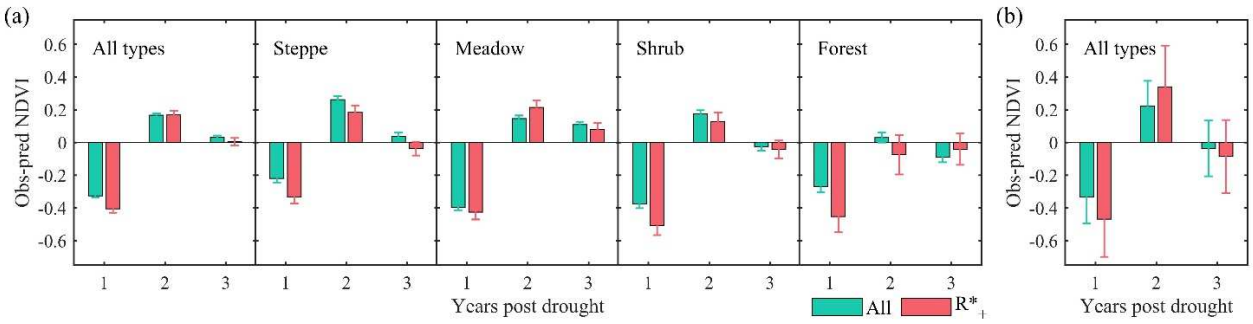

Fig. 3. Drought legacy effects of growing season NDVI in grids (a) and meteorological sites (b) at periods of 1~3 years after extreme drought events over the TP. Turquoise and pink bars show results from all grids/sites (All) and grids/sites with significant and positive correlation (R^*_+) between NDVI and SPEI. Error bars

represent 95% confidence intervals around the mean from 1,000 bootstrapped estimates.

3.2. Spatial patterns of legacy effects for one year after extreme drought events

The spatial patterns of the correlation coefficients between $NDVI_{GS}$ and drought variables and the legacy effects in the first year after severe drought are mapped in Figure 4. Overall, the $NDVI_{GS}$ showed stronger relationships with the SPEI than with the CWD (Fig. 4a and Fig. A3a). Significant positive correlations between the $NDVI_{GS}$ and the two drought variables were observed over ~15% and ~20% of the study area, with a mean Pearson's correlation coefficient of approximately 0.45 for both drought variables. On the other hand, approximately 37% and 43% of the meteorological sites showed significant positive correlations with CWD and SPEI, respectively. There were consistent spatial patterns of the correlation coefficients between the grid points and sites. Regions of significant positive coefficients appeared mainly on the southwestern and northeastern plateau and in the Yangtze River basin (Fig. 4a), indicating a substantial dependence of vegetation growth on water availability in these regions. $NDVI_{GS}$ in parts of the southern, southeastern and central plateau exhibited negative correlations with drought variables (Fig. 4a and Fig. A3a). These negative relationships also occurred in the partial correlation analysis by controlling the mean growing season temperature (Fig. A4), suggesting that the interannual variations in vegetation growth in these regions are unlikely constrained by water stress but were probably driven by variations in insolation because less precipitation may suggest fewer cloudy days and

297 more insolation, which can positively affect plant growth over these regions (Zhang et
298 al., 2017).

299 Negative drought legacy effects were prevalent across most parts (~70% of the
300 study area) of the TP, irrespective of the relationship between $NDVI_{GS}$ and water
301 deficits (Fig. 4b). The SPEI-based legacy effects were largely consistent with those
302 derived from CWD (Fig. 4b and Fig. A3b), as well as with those derived from
303 residuals of the $NDVI_{GS}$ after removing the effects of temperature by linear regression
304 (Fig. A4). Note that the validity of the legacy effects depended on the strength of the
305 regression between $NDVI_{GS}$ and drought variables. Therefore, we focused on regions
306 where $NDVI_{GS}$ was significantly positively correlated with drought stress. In these
307 regions, vegetation greenness exhibited pronounced negative legacy effects (~71% of
308 the pixels with significant positive NDVI-SPEI relationships) (Fig. 4b and Fig. A3b).
309 Positive legacy effects (~29%), where observed $NDVI_{GS}$ increased compared to that
310 predicted in the next year, were sparsely located in the central, western, and humid
311 forest regions on the eastern edges of the plateau (Fig. 4b).

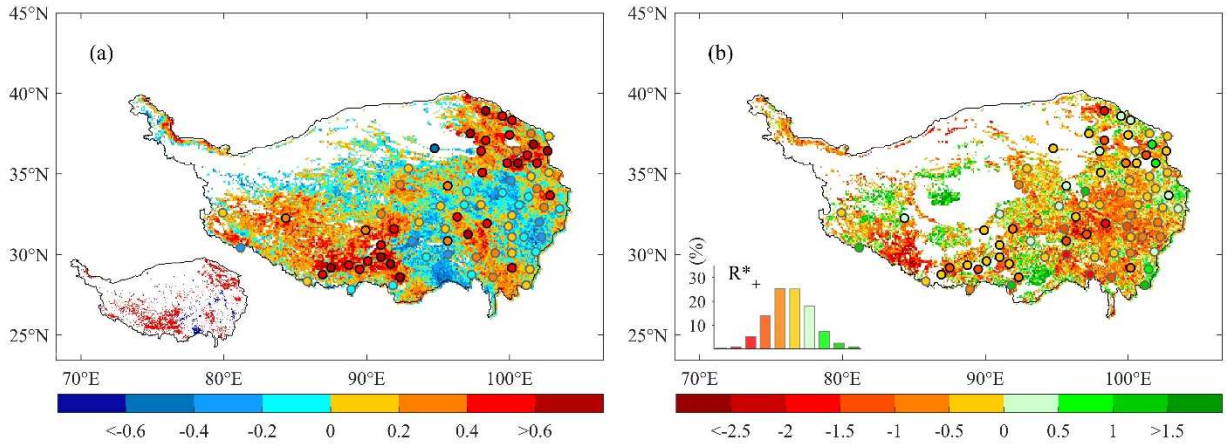

312

313 **Fig. 4.** Spatial patterns of correlation coefficients between growing season NDVI and

SPEI (a), and the legacy effect in the first year post-drought derived from SPEI (b). Colors of circles show results from meteorological sites (circles with black edges represent sites with significant correlation between NDVI and SPEI, $p < 0.05$). Inset in (a) shows the pixels with significant NDVI-SPEI relationships (red: positive, blue: negative). Inset in (b) shows the frequency histogram of the legacies across pixels with significant positive NDVI-SPEI relationships (R^*_+) in (a). Extra blank areas in (b) means that no extreme drought event is detected during 1982−2015.

3.3. Elevation-dependent differences in legacy effects between different ecosystem types

The magnitude of vegetation greenness legacy effects in the first year after extreme drought showed clear altitude dependencies over the TP. Figure 5 shows the changes in legacy effects along the elevational gradient (at 100 m interval bins). For all PFGs combined, the negative drought legacy effects deduced from the SPEI and CWD showed a significant increasing trend along the elevational gradients (Fig. 5a and Fig. A5a). For the alpine steppe, the magnitude of negative drought legacy effects gradually increased from 0.2 in 2200 m to 0.9 in 3800 m ($p < 0.001$), then decreased with elevation ($p < 0.001$), reaching approximately 0.09 at 5200 m, and then changed to positive legacy effects at bins of 5300 m and 5400 m (Fig. 5b). In contrast, the alpine meadow showed an increasing magnitude of negative legacy effect along the elevation bins of 3200-5400 m ($p = 0.05$, Fig. 5c). This increasing trend was more evident after removing the effects of temperature ($p < 0.01$), particularly at altitudes

higher than 4000 m, with the largest legacy effect of approximately 1 at 5300 m (Fig. A5c). The contrasting elevation dependencies of steppe and meadow at higher altitudes were robust regardless of the different data used or whether the effect of temperature was removed (Fig. A5). Shrub showed a weak decreasing trend in negative legacy effects with altitude (p = 0.05, Fig. 5d), whereas this trend did not exist after removing the effects of temperature or when using CWD data (Fig. A5d), which should be treated with caution because of the possibility of inaccurate remote sensing data due to the complex and steep terrain of shrublands (Fig. 1). Drought legacy effects on the greenness of forest did not show significant trends with altitude (Fig. 5).

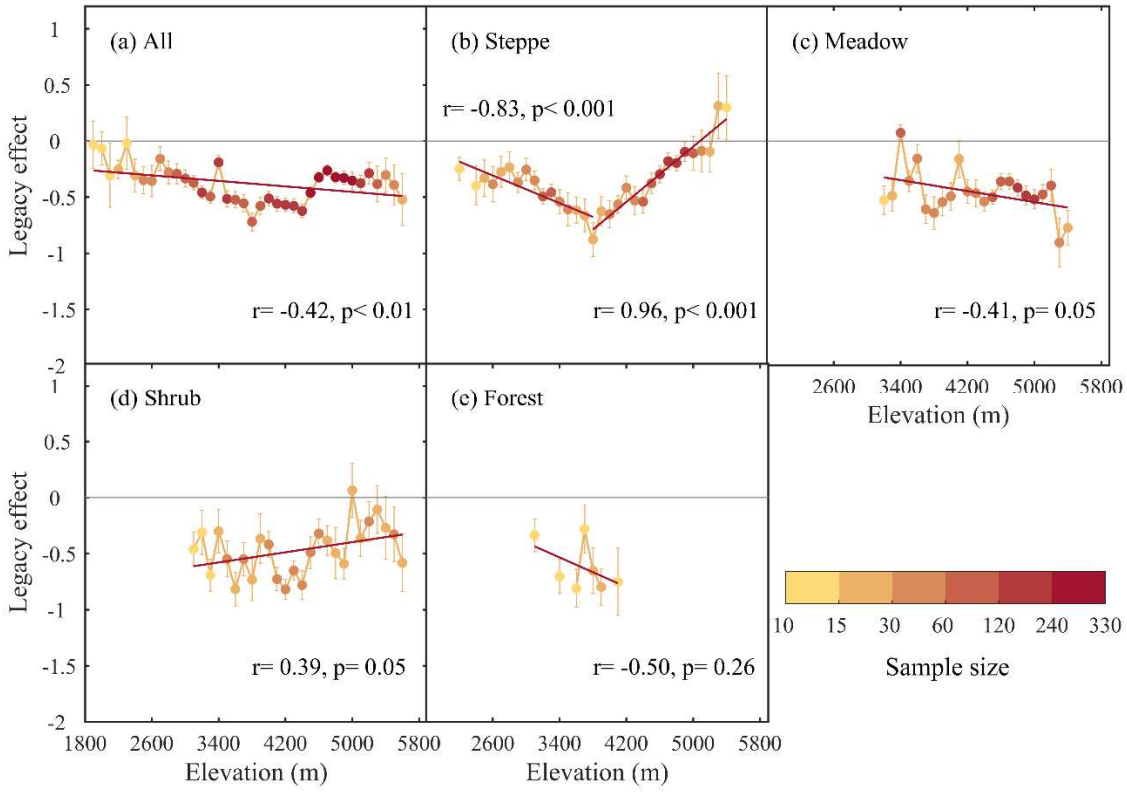

Fig. 5. Relationship between legacy effect on growing season NDVI in the first year after drought events and elevation (at 100m interval bins). Only pixels with significant

and positive correlation between growing season NDVI and SPEI and bins with at least 10 sample size were included in the analysis. Dots illustrate the average values within the corresponding elevation bins. Error bars represent 95% confidence intervals around the mean from 1,000 bootstrapped estimates.

4. Discussion

4.1. Consistent drought legacy effects on plant growth among different PFGs on the TP

Unexpectedly similar durations of drought legacy effects on growing-season vegetation greenness among different PFGs on the TP may be linked to the limited resource availability and adaptive response of plant growth to drought conditions in alpine environments (Liu et al., 2019; Marine et al., 2015). In general, temperate herbaceous grassland species can recover very rapidly in the following growing season after drought through efficient root water use patterns and interspecific functional strategies (Dreesen et al., 2014; Griffin-Nolan et al., 2018; Hoover et al., 2014; Lloret et al., 2012). However, pervasive incomplete growth in the year after extreme drought and lagged recovery until the second year were observed in TP grasslands (Fig. 2 and Fig. 3). The result that vegetation growth continued to be suppressed in the following year has also been found in other semi-arid grasslands (Arredondo et al., 2016). When extreme drought combines with heat, i.e., 'hot drought', the legacy effect can occur for up to 2 years in alpine grasslands (De Boeck et al., 2018). The observed legacy effects after drought on the TP and other alpine grasslands might be attributable to low nutrient availability in soil and the phenological constraints that limit potential

368 growth later in the growing season (Cremonese et al., 2017; De Boeck et al., 2016;
369 Zhang et al., 2019a). Relatively lower soil water availability could suppress soil
370 nutrient cycling, leading to nutrient deficiencies in plants and microbes (Aanderud et
371 al., 2010; Wang et al., 2013a), which may modulate the response of alpine grasslands
372 to drought. On the other hand, unlike annual grass that can quickly colonize open
373 niches in the following growing season, the dominant plant species of perennials on
374 the TP may be subject to slower recruitment and thus delayed recovery from drought,
375 especially under a shorter growing season than that of temperate grasslands and alpine
376 conditions that make seedling establishment more difficult (De Boeck et al., 2018).
377 Moreover, for perennials, drought legacy effects may arise from changes in structural
378 components such as a reduced tiller density that can limit recruitment of new tillers and
379 maximum leaf area in the next year after drought and stolon density that can restrict the
380 regeneration process through a stoloniferous expansion strategy (Reichmann and Sala,
381 2014; Reichmann et al., 2013).

382 The one-year drought legacy effect on shrub growth in our study is consistent with
383 that from field experiments, which have shown an approximate drought legacy effect
384 of 1~2 years (Jobbágy and Sala, 2000). However, tree-ring chronologies in temperate
385 and boreal forest ecosystems have shown longer drought legacy effects than that
386 based on forest NDVI in the TP in this study. Since NDVI is a proxy for canopy
387 greenness while tree-ring widths indicate stem radial growth, such difference may be
388 partly explained by the dynamic carbon allocation strategies of forest ecosystems in
389 response to drought with a preferential allocation to the canopy as opposed to wood,

390 leading to longer legacy effects in tree rings than in NDVI (Kannenberg et al., 2019b;
391 Kannenberg et al., 2020). In addition, the carbon allocation mechanism after drought
392 also varies across different biomes (Gazol et al., 2018). Moreover, acclimation
393 mechanisms in semi-arid forests coping with drought could also be one potential
394 mechanism underlying a more rapid recovery after drought in woody plants on the
395 plateau (Fang and Zhang, 2019; Liu et al., 2008). Our results suggest that tree growth
396 on the TP is unlikely to have experienced severe hydraulic damage or extensive
397 mortality, which could otherwise lead to years of recovery after extreme drought
398 events.

399 It is, however, difficult to compare drought legacy effects across the globe due to
400 various quantitative approaches based on radial growth, remote sensing products and
401 leaf-level observations, and varied definitions of drought events that contribute to the
402 reported highly variable legacy effects in terms of duration and magnitude
403 (Kannenberg et al., 2020). On the Tibetan Plateau, although vegetation greenness
404 showed similar durations and comparable magnitudes of drought legacy effects among
405 different PFGs at a regional scale (Fig. 3), the magnitude of legacy effects exhibited
406 large spatial heterogeneity (Fig. 4). Thus, our study highlights the need for further
407 research into the physiological and ecological mechanisms of alpine vegetation in
408 response to extreme drought events.

409 4.2. Divergent changes in elevational gradients of drought legacy effects between
410 alpine meadow and steppe

411 The drought legacy effects on vegetation greenness varied with altitude, which
412 may have been due to altitudinal shifts in climate factors limiting plant recovery
413 among different ecosystem types. In the alpine meadow areas, the magnitude of
414 negative legacy effects increased with altitude (Fig. 5c and Fig. A5c), coincident with
415 a reverse dependence on temperature and water availability ($p < 0.05$) (Fig. 6e-g and
416 Fig. A6), which suggests a more pronounced negative legacy effect under relatively
417 drier and colder conditions. It has been documented that for forest ecosystems, the
418 magnitude of the legacy effect is associated with precipitation but nonsignificantly
419 correlated with temperature (Anderegg et al., 2015b). For the alpine meadow on the
420 TP, both water availability and thermal conditions appeared to impact the drought
421 legacy effect and thus its resilience to drought, probably linked to the dual limitation
422 of temperature and precipitation on TP grassland productivity (Liu et al., 2018). In
423 addition, it has been documented that vegetation growth has relatively higher climate
424 sensitivity at higher altitudes (Li et al., 2019a; Tao et al., 2015; Wang et al., 2013b);
425 therefore, the declining water availability and air temperature concurrent with the
426 increasing sensitivity of growth to climate at higher elevations may result in an
427 amplified reduction in $NDVI_{GS}$ at higher altitudes over the TP. Apart from climate
428 factors, soil hydraulic properties, particularly soil water holding capacity (WHC) that
429 is determined by soil texture and organic content (Dai et al., 2013b), might also
430 impact the magnitude of drought legacy effect and thus contribute to the observed

elevation-dependence of the legacy effect. However, our analysis shows that WHC is not significantly correlated with the legacy effect for alpine meadow (Fig. A7).

Drought-induced legacy effects in the alpine steppe increased at lower altitudes (lower than 3800 m) and then decreased sharply at higher altitudes (higher than 3800 m), showing an opposite trend in elevation dependence to that of the meadow. In contrast to the alpine meadow, the magnitude of the negative legacy effects in the alpine steppe was positively related to precipitation and water deficit ($p < 0.001$, Fig. 6a,b), i.e. the drier the region, the smaller the magnitude of the negative legacy effect was. Therefore, the segmented trends between lower and higher altitudes (Fig. 5b) might be linked to the different changes in precipitation between lower and higher elevations (Fig. A6). As for the potential impact of soil hydraulic properties, although soil WHC is negatively correlated with the legacy effect, the relationship becomes non-significant when CWD (or precipitation) is controlled for (Fig. A7). Thus, the long-term water availability, rather than WHC, may be an important factor that influences the drought legacy effect in alpine steppe over the TP. We speculate that compared with the semi-arid meadow, the steppe ecosystem on the TP evolved ecophysiological traits adapted to arid environments, leading to higher resilience associated with higher water-use efficiency (Ponce-Campos et al., 2013; Wu et al., 2013); thus, steppes generally have a smaller magnitude of legacy effects compared to that of meadows (Fig. 3), albeit with lower precipitation and water availability (Fig. A6). The positive relationship between the drought legacy effect and precipitation in alpine steppe might be attributable to the negative correlation between water-use

efficiency and precipitation (Huang et al., 2015; Wu et al., 2013), whereby a higher water-use efficiency enables growth with less water, possibly conferring a relatively more rapid recovery rate after drought. However, further research is needed to clarify this mechanism.

Accordingly, we argue here that the large spatial heterogeneity in the drought legacy effects across the TP is likely attributable to different hydrothermal conditions caused by elevational gradients and the diverse response strategies of different ecosystem types. Other climatic factors that depend on elevation, such as sunshine duration and terrain slope angle, may also lead to changes in vegetation recovery. The widespread long-lasting post-drought effects across the TP, particularly on the southwestern and northeastern plateau where vegetation growth is highly dependent on water availability, indicate a high risk of grassland degradation induced by the projected increasing extreme drought events in the future, which may affect hydrological and ecological services in Asia.

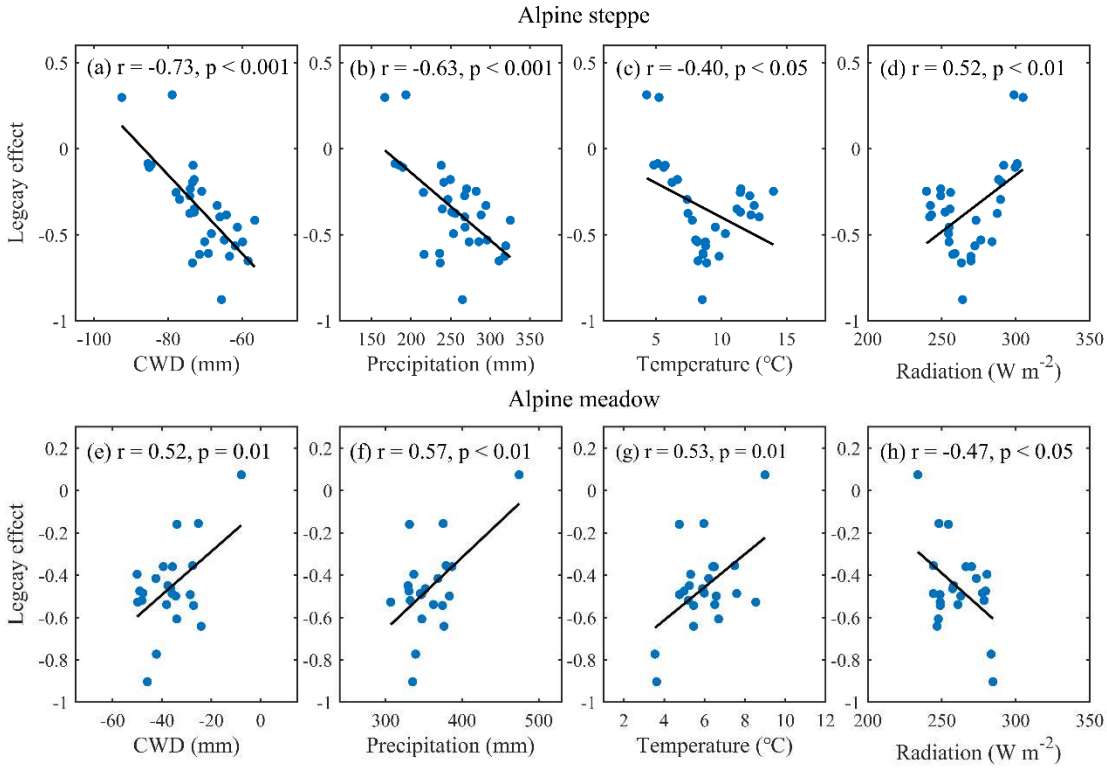

Fig. 6. Relationships between legacy effects on growing season NDVI in the first year post-drought events and multi-year mean growing season climatic water deficit (CWD), precipitation, temperature and downward shortwave radiation in alpine steppe and meadow. Dots represent average values within the 100m elevation bins. Only pixels with significant and positive NDVI-SPEI relationships were included in each elevation bin, and only bins with at least 10 sample size are shown here.

5. Conclusions

In this study, we detected prevalent legacy effects on growing-season vegetation greenness in the first year after extreme drought events in alpine ecosystems of the TP. That is, albeit with climatic conditions returning to normal after drought, plants did not recover their expected growth for approximately one year, regardless of ecosystem

types. To our knowledge, our study is the first to reveal the drought legacy effects on greenness over the alpine ecosystems of the TP at a regional scale. Importantly, the same lag time and comparable magnitude of legacy effects among grass, shrubs, and forests are observed on the plateau. Meanwhile, drought legacy effects are spatially heterogeneous and exhibit clear altitude dependence, while divergent relationships between altitude and the magnitude of reduced $NDVI_{GS}$ in the first year post-drought are observed between alpine steppe and meadow. For alpine meadow, the negative legacy effects are more pronounced at higher altitudes with reduced precipitation and temperature, indicating a weaker drought resilience under dryer and colder conditions. In contrast, for alpine steppe, smaller legacy effects are found in regions with lower precipitation, suggesting a stronger drought resilience of plant communities in dryer regions for alpine steppe. Thus, the distinct elevation dependencies of drought legacy effects may be attributable to altitudinal shifts in climate factors that limit plant growth and to different strategies among ecosystem types to cope with droughts. More observations and in situ experiments on vegetation recovery after drought are needed to further explore the mechanisms underlying the varying responses to drought on the TP, probably involving vertical changes in plant physiological traits, species distribution and community structure. The results from this study help improve our knowledge of vegetation vulnerability to extreme droughts in alpine ecosystems. Given the rapid climate change over the TP with a projected increasing trend in the frequency and intensity of extreme events in both temperature and precipitation (You et al., 2020), the identified widespread drought legacy effects demonstrate the

necessity to account for the potential prolonged effects of extreme climate events in order to better predict future ecosystem dynamics and functions on the TP.

Acknowledgements

We would like to thank the constructive suggestions from Dr. Ying Deng when preparing the manuscript. This study was jointly supported by the National Natural Science Foundation of China [grant numbers 41861134036, 41988101], and the Second Tibetan Plateau Scientific Expedition and Research Program [grant number 2019QZKK0405].

References

Aanderud, Z.T., Richards, J.H., Svejcar, T. and James, J.J., 2010. A shift in seasonal rainfall reduces soil organic carbon storage in a cold desert. Ecosystems, 13(5): 673-682.Allen, C.D., Breshears, D.D. and McDowell, N.G., 2015. On underestimation of global vulnerability to tree mortality and forest die‐off from hotter drought in the Anthropocene. Ecosphere, 6(8): 1-55.

Anderegg, W.R. et al., 2015a. Tree mortality from drought, insects, and their interactions in a changing climate. New Phytol., 208(3): 674-683.

Anderegg, W.R. et al., 2015b. Pervasive drought legacies in forest ecosystems and their implications for carbon cycle models. Science, 349(6247): 528-532.

Anderegg, W.R.L. et al., 2016. Meta-analysis reveals that hydraulic traits explain cross-species patterns of drought-induced tree mortality across the globe. Proc. Natl. Acad. Sci. U.S.A., 113(18): 5024.

Arredondo, T. et al., 2016. Drought manipulation and its direct and legacy effects on productivity of a monodominant and mixed-species semi-arid grassland. Agric. For. Meteorol., 223: 132-140.

Barichivich, J. et al., 2013. Large-scale variations in the vegetation growing season and annual cycle of atmospheric CO_2 at high northern latitudes from 1950 to 2011. Global Change Biol., 19(10): 3167-3183.

Beguería, S., Vicente‐Serrano, S.M., Reig, F. and Latorre, B., 2014. Standardized precipitation evapotranspiration index (SPEI) revisited: parameter fitting, evapotranspiration models, tools, datasets and drought monitoring. Int. J.

Climatol., 34(10): 3001-3023.

Brando, P.M. et al., 2014. Abrupt increases in Amazonian tree mortality due to drought–fire interactions. Proc. Natl. Acad. Sci. U.S.A., 111(17): 6347-6352.

Bréda, N., Huc, R., Granier, A. and Dreyer, E., 2006. Temperate forest trees and stands under severe drought: a review of ecophysiological responses, adaptation processes and long-term consequences. Ann. For. Sci., 63(6): 625-644.

Camarero, J.J., Gazol, A., Sangüesa‐Barreda, G., Oliva, J. and Vicente‐Serrano, S.M., 2015. To die or not to die: early warnings of tree dieback in response to a severe drought. J. Ecol., 103(1): 44-57.

Chen, Y. et al., 2011. Improving land surface temperature modeling for dry land of China. J. Geophys. Res. Atmos., 116(D20).

Chen, N. et al., 2020. The compensation effects of post-drought regrowth on earlier drought loss across the tibetan plateau grasslands. Agric. For. Meteorol., 281: 107822.

Ciais, P. et al., 2005. Europe-wide reduction in primary productivity caused by the heat and drought in 2003. Nature, 437(7058): 529-533.

Cremonese, E. et al., 2017. Heat wave hinders green wave: The impact of climate extreme on the phenology of a mountain grassland. Agric. For. Meteorol., 247: 320-330.

Cui, X. and Graf, H.-F., 2009. Recent land cover changes on the Tibetan Plateau: a review. Clim. Change, 94(1-2): 47-61.

Dai, A., 2013a. Increasing drought under global warming in observations and models. Nat. Clim. Change, 3(2): 171-171.

Dai, Y., et al., 2013b: Development of a China dataset of soil hydraulic parameters using pedotransfer functions for land surface modeling. J. Hydrometeorol., 14: 869-887.

De Boeck, H.J., Bassin, S., Verlinden, M., Zeiter, M. and Hiltbrunner, E., 2016. Simulated heat waves affected alpine grassland only in combination with drought. New Phytol., 209(2): 531–541.

De Boeck, H.J., Hiltbrunner, E., Verlinden, M., Bassin, S. and Zeiter, M., 2018. Legacy effects of climate extremes in alpine grassland. Front. Plant Sci., 9: 1586.

Dreesen, F.E., De Boeck, H.J., Janssens, I.A. and Nijs, I., 2014. Do successive climate extremes weaken the resistance of plant communities? An experimental study using plant assemblages. Biogeosciences, 11(1): 109-121.

Duan, A. and Wu, G., 2005. Role of the Tibetan Plateau thermal forcing in the summer climate patterns over subtropical Asia. Clim. Dyn., 24(7-8): 793-807.

Fang, O. and Zhang, Q.B., 2019. Tree resilience to drought increases in the Tibetan Plateau. Global Change Biol., 25(1): 245-253.

Fu, G. et al., 2013. Experimental warming does not enhance gross primary production and above-ground biomass in the alpine meadow of Tibet. J. Appl. Remote Sens., 7(1): 073505.

575 Gazol, A., Camarero, J., Anderegg, W. and Vicente‐Serrano, S., 2017. Impacts of
576 droughts on the growth resilience of Northern Hemisphere forests. Global.
577 Ecol. Biogeogr, 26(2): 166-176.
578 Gazol, A. et al., 2018. Forest resilience to drought varies across biomes. Global
579 Change Biol. , 24(5): 2143-2158.
580 Griffin-Nolan, R.J. et al., 2018. Legacy effects of a regional drought on aboveground
581 net primary production in six central US grasslands. Plant Ecol., 219(5):
582 505-515.
583 [dataset] He, J. et al., 2020. The first high-resolution meteorological forcing dataset
584 for land process studies over China. Scientific Data, 7, 25,
585 https://doi.org/10.1038/s41597-020-0369-y.
586 Hoover, D.L., Knapp, A.K. and Smith, M.D., 2014. Resistance and resilience of a
587 grassland ecosystem to climate extremes. Ecology, 95(9): 2646-2656.
588 Huang, J. et al., 2017a. Dryland climate change: Recent progress and challenges. Rev.
589 Geophys., 55(3): 719-778.
590 Huang, M. et al., 2019. Air temperature optima of vegetation productivity across
591 global biomes. Nat. Ecol. Evol., 3(5): 772-779.
592 Huang, M. et al., 2015. Change in terrestrial ecosystem water‐use efficiency over the
593 last three decades. Global Change Biol., 21(6): 2366-2378.
594 Huang, M. et al., 2017b. Velocity of change in vegetation productivity over northern
595 high latitudes. Nat. Ecol. Evol., 1(11): 1649-1654.
596 Huang, M., Wang, X., Keenan, T.F. and Piao, S., 2018. Drought timing influences the

legacy of tree growth recovery. Global Change Biol., 24(8): 3546-3559.

IPCC et al., 2013. Climate Change 2013: The Physical Science Basis: Working Group I Contribution to the Fifth Assessment Report of the Intergovernmental Panel on Climate Change. Cambridge University Press Cambridge, UK.

Itter, M.S. et al., 2019. Boreal tree growth exhibits decadal‐scale ecological memory to drought and insect defoliation, but no negative response to their interaction. J. Ecol., 107(3): 1288-1301.

Jobbágy, E.G. and Sala, O.E., 2000. Controls of grass and shrub aboveground production in the Patagonian steppe. Ecol. Appl., 10(2): 541-549.

Jorge, P. and Compton, T., 2014. A Non-Stationary 1981–2012 AVHRR NDVI3g Time Series. Remote Sens., 6(8): 6929-6960.

Kannenberg, S.A. et al., 2019a. Drought legacies are dependent on water table depth, wood anatomy and drought timing across the eastern US. Ecol. Lett., 22(1): 119-127.

Kannenberg, S.A. et al., 2019b. Linking drought legacy effects across scales: From leaves to tree rings to ecosystems. Global Change Biol., 25(9): 2978-2992.

Kannenberg, S.A., Schwalm, C.R. and Anderegg, W.R., 2020. Ghosts of the past: how drought legacy effects shape forest functioning and carbon cycling. Ecol. Lett., 23(5): 891-901.

Li, L. et al., 2019a. Increasing sensitivity of alpine grasslands to climate variability along an elevational gradient on the Qinghai-Tibet Plateau. Sci. Total. Environ., 678: 21-29.

Li, P., Hu, Z. and Liu, Y., 2020. Shift in the trend of browning in Southwestern Tibetan Plateau in the past two decades. Agric. For. Meteorol., 287: 107950.

Li, X. et al., 2019b. The impact of the 2009/2010 drought on vegetation growth and terrestrial carbon balance in Southwest China. Agric. For. Meteorol., 269: 239-248.

Liang, E., Leuschner, C., Dulamsuren, C., Wagner, B. and Hauck, M., 2015. Global warming-related tree growth decline and mortality on the north-eastern Tibetan plateau. Clim. Change, 134(1-2): 163-176.

Liang, S. et al., 2013a. Global LAnd Surface Satellite (GLASS) products: algorithms, validation and analysis. Springer, New York.

[dataset] Liang, S. et al., 2013b. A long-term Global LAnd Surface Satellite (GLASS) data-set for environmental studies. INT J DIGIT EARTH, 6(sup1): 5-33. https://doi.org/10.1080/17538947.2013.805262.

Liu, D. et al., 2018. Contrasting responses of grassland water and carbon exchanges to climate change between Tibetan Plateau and Inner Mongolia. Agric. For. Meteorol., 249: 163-175.

Liu, D. et al., 2019. Deciphering impacts of climate extremes on Tibetan grasslands in the last fifteen years. Chin. Sci. Bull., 64(7): 446-454.

Liu, X. et al., 2008. Response and dendroclimatic implications of $\delta^{13}C$ in tree rings to increasing drought on the northeastern Tibetan Plateau. J. Geophys. Res. Biogeosci., 113(G3): G03015.

Lloret, F., Escudero, A., Iriondo, J.M., Martínez‐Vilalta, J. and Valladares, F., 2012.

641 Extreme climatic events and vegetation: the role of stabilizing processes.
642 Global Change Biol., 18(3): 797-805.
643 Marine, Z., Catherine, P.C., Annette, M.B., Marie-Pascale, P.h. and Florence, V., 2015.
644 What functional strategies drive drought survival and recovery of perennial
645 species from upland grassland? Ann. Bot., 116(6): 1001-1015.
646 Mcdowell, N.G. et al., 2008. Mechanisms of plant survival and mortality during
647 drought: why do some plants survive while others succumb to drought? New
648 Phytol., 178(4): 719-739.
649 Monteith, J.L., 1965. Evaporation and environment, Symposia of the society for
650 experimental biology. Cambridge University Press (CUP) Cambridge, pp.
651 205-234.
652 Ogle, K. et al., 2015. Quantifying ecological memory in plant and ecosystem
653 processes. Ecol. Lett., 18(3): 221-235.
654 Pederson, N. et al., 2014. The legacy of episodic climatic events in shaping temperate,
655 broadleaf forests. Ecol. Monogr., 84(4): 599-620.
656 Peltier, D.M., Fell, M. and Ogle, K., 2016. Legacy effects of drought in the
657 southwestern United States: A multi‐species synthesis. Ecol. Monogr., 86(3):
658 312-326.
659 Piao, S. et al., 2011. Altitude and temperature dependence of change in the spring
660 vegetation green-up date from 1982 to 2006 in the Qinghai-Xizang Plateau.
661 Agric. For. Meteorol., 151(12): 1599-1608.
662 Piao, S. et al., 2014. Evidence for a weakening relationship between interannual

temperature variability and northern vegetation activity. Nat. Commun., 5: 5018.

Piao, S. et al., 2019a. Characteristics, drivers and feedbacks of global greening. Nat. Rev. Earth Environ., 1-14.

Piao, S. et al., 2019b. The impacts of climate extremes on the terrestrial carbon cycle: A review. Sci. China: Earth Sci., 62(10): 1551-1563.

Piao, S. et al., 2019c. Responses and feedback of the Tibetan Plateau's alpine ecosystem to climate change. Chin. Sci. Bull., 64(27): 2842-2855.

Ponce-Campos, G.E. et al., 2013. Ecosystem resilience despite large-scale altered hydroclimatic conditions. Nature, 494(7437): 349-352.

Ramsey, F.L., 1974. Characterization of the partial autocorrelation function. Ann. Stat., 2(6): 1296-1301.

Reichmann, L.G. and Sala, O.E., 2014. Differential sensitivities of grassland structural components to changes in precipitation mediate productivity response in a desert ecosystem. Funct. Ecol., 28(5): 1292-1298.

Reichmann, L.G., Sala, O.E. and Peters, D.P., 2013. Precipitation legacies in desert grassland primary production occur through previous‐year tiller density. Ecology, 94(2): 435-443.

Sala, O.E., Gherardi, L.A., Reichmann, L., Jobbágy, E. and Peters, D., 2012. Legacies of precipitation fluctuations on primary production: theory and data synthesis. Phil. Trans. R. Soc. B, 367(1606): 3135-3144.

Scheffer, M. et al., 2009. Early-warning signals for critical transitions. Nature,

461(7260): 53-59.

Schewe, J. et al., 2019. State-of-the-art global models underestimate impacts from climate extremes. Nat. Commun., 10(1): 1-14.

Schwalm, C.R. et al., 2017. Global patterns of drought recovery. Nature, 548(7666): 202-205.

Seidl, R. et al., 2018. Invasive alien pests threaten the carbon stored in Europe's forests. Nat. Commun., 9(1): 1-10.

Sheffield, J., Wood, E.F. and Roderick, M.L., 2012. Little change in global drought over the past 60 years. Nature, 491(7424): 435-438.

Stephenson, N., 1998. Actual evapotranspiration and deficit: biologically meaningful correlates of vegetation distribution across spatial scales. J. Biogeogr., 25(5): 855-870.

Tao, J., Zhang, Y., Dong, J., Fu, Y. and Xi, Y., 2015. Elevation-dependent relationships between climate change and grassland vegetation variation across the Qinghai-Xizang Plateau. Int. J. Climatol., 35(7): 1638-1647.

Vicente-Serrano, S.M., Beguería, S. and López-Moreno, J.I., 2010. A multiscalar drought index sensitive to global warming: the standardized precipitation evapotranspiration index. J. Clim., 23(7): 1696-1718.

Vicente-Serrano, S.M. et al., 2013. Response of vegetation to drought time-scales across global land biomes. Proc. Natl. Acad. Sci. U.S.A., 110(1): 52-57.

Wang, Z.-y., Sun, G., Luo, P., Mou, C.-x. and Wang, J., 2013a. A study of soil-dynamics based on a simulated drought in an alpine meadow on the

Tibetan Plateau. J MT SCI-ENGL, 10(5): 833-844.

Wang, Z., Luo, T., Li, R., Tang, Y. and Du, M., 2013b. Causes for the unimodal pattern of biomass and productivity in alpine grasslands along a large altitudinal gradient in semi-arid regions. J. Veg. Sci., 24(1): 189-201.

Wu, J. et al., 2013. Grazing-exclusion effects on aboveground biomass and water-use efficiency of alpine grasslands on the Northern Tibetan Plateau. Rangeland Ecol. Manage., 66(4): 454-461.

Wu, X. et al., 2017. Differentiating drought legacy effects on vegetation growth over the temperate Northern Hemisphere. Global Change Biol., 24(1): 504-516.

Xu, C. et al., 2019. Increasing impacts of extreme droughts on vegetation productivity under climate change. Nat. Clim. Change, 9(12): 948-953.

Yang, K., He, J., Tang, W., Qin, J. and Cheng, C.C., 2010. On downward shortwave and longwave radiations over high altitude regions: Observation and modeling in the Tibetan Plateau. Agric. For. Meteorol., 150(1): 38-46.

Yao, T. et al., 2019. Recent Third Pole's rapid warming accompanies cryospheric melt and water cycle intensification and interactions between monsoon and environment: Multidisciplinary approach with observations, modeling, and analysis. Bull. Am. Meteorol. Soc., 100(3): 423-444.

You, Q. et al., 2020. Tibetan Plateau amplification of climate extremes under global warming of 1.5 °C, 2 °C and 3 °C. Glob. Planet. Change. 192, 103261.

Zhang, Q., Kong, D., Singh, V.P. and Shi, P., 2017. Response of vegetation to different time-scales drought across China: Spatiotemporal patterns, causes and

729 implications. Global Planet. Change, 152: 1-11.
730 Zhang, T. et al., 2018. Water availability is more important than temperature in driving
731 the carbon fluxes of an alpine meadow on the Tibetan Plateau. Agric. For.
732 Meteorol., 256: 22-31.
733 Zhang, X.-Z., Shen, Z.-X. and Fu, G., 2015. A meta-analysis of the effects of
734 experimental warming on soil carbon and nitrogen dynamics on the Tibetan
735 Plateau. Appl. Soil Ecol., 87: 32-38.
736 Zhang, Y., Huang, K., Zhang, T., Zhu, J. and Di, Y., 2019a. Soil nutrient availability
737 regulated global carbon use efficiency. Global Planet. Change, 173: 47-52.
738 Zhang, Y., Zhu, Y., Li, J. and Chen, Y., 2019b. Current status and future directions of
739 the Tibetan Plateau ecosystem research. Chin. Sci. Bull., 64(7): 428-430.
740 Zhu, Z. et al., 2016. Greening of the Earth and its drivers. Nat. Clim. Change, 6(8):
741 791-795.
742

Appendices

Figs. A1-A7.

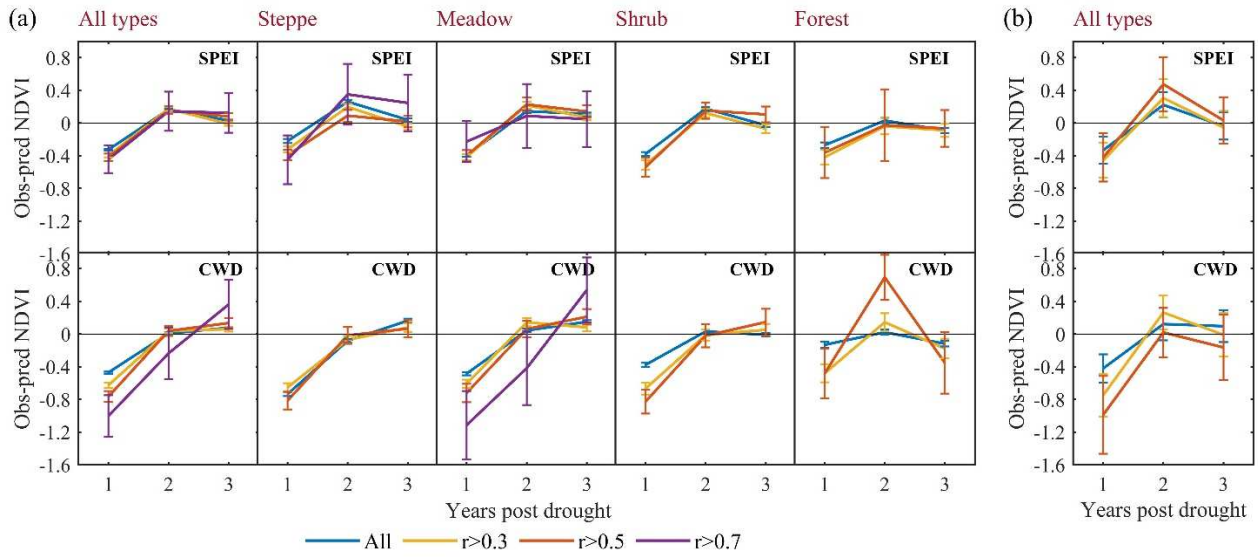

Fig. A1. Drought legacy effects on growing season NDVI derived from SPEI and CWD in grids (a) and meteorological sites (b) at periods of 1~3 years after extreme drought events over the TP. Only results with at least 10 sample size were included in the analysis. Error bars represent 95% confidence intervals around the mean from 1,000 bootstrapped estimates.

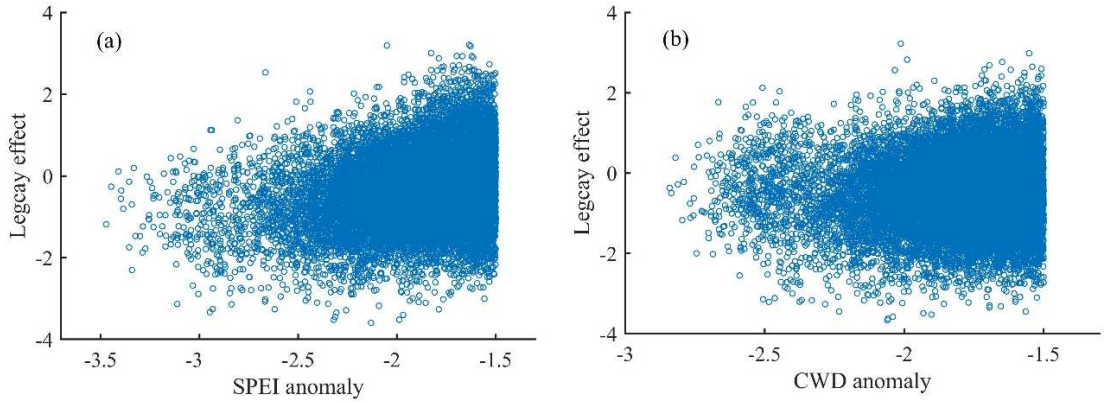

Fig. A2. Relationship between the legacy effects in growing season NDVI after the first year drought events and anomaly of SPEI (a), CWD (b).

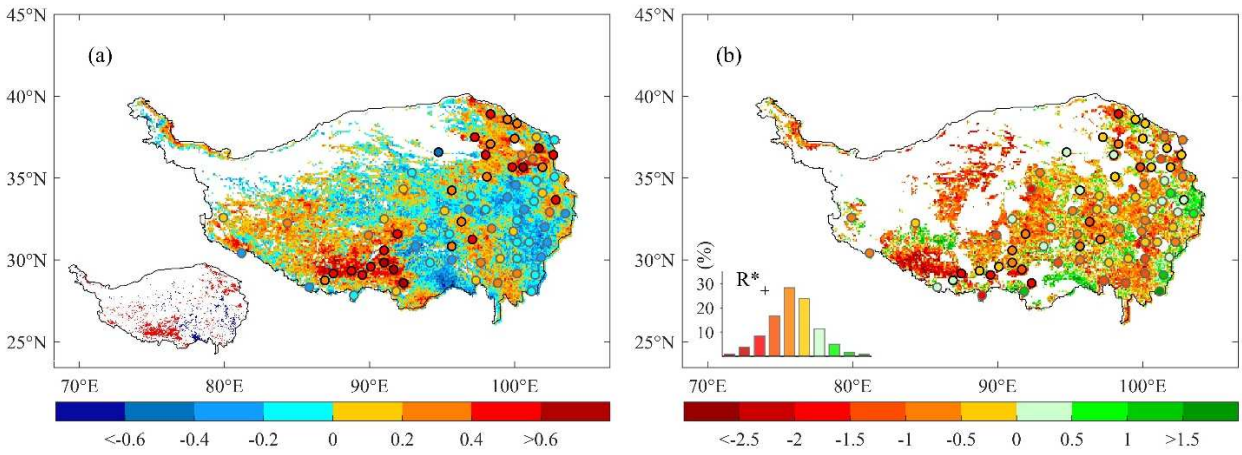

754

755 **Fig. A3.** Spatial patterns of correlation coefficients between growing season NDVI
756 and CWD (a), and the legacy effect in the first year post-drought derived from CWD
757 (b). Colors of circles show results from meteorological sites (circles with black edges
758 represent sites with significant and positive correlation between NDVI and CWD, $p <$
759 0.05). Inset in (a) shows the pixels with significant NDVI-CWD relationships (red:
760 positive, blue: negative). Inset in (b) shows the frequency histogram of the legacy
761 effects across pixels with significant positive NDVI-CWD relationships (R^*_+) in (a).
762 Extra blank areas in (b) means that no extreme drought event is detected during
763 1982-2015.

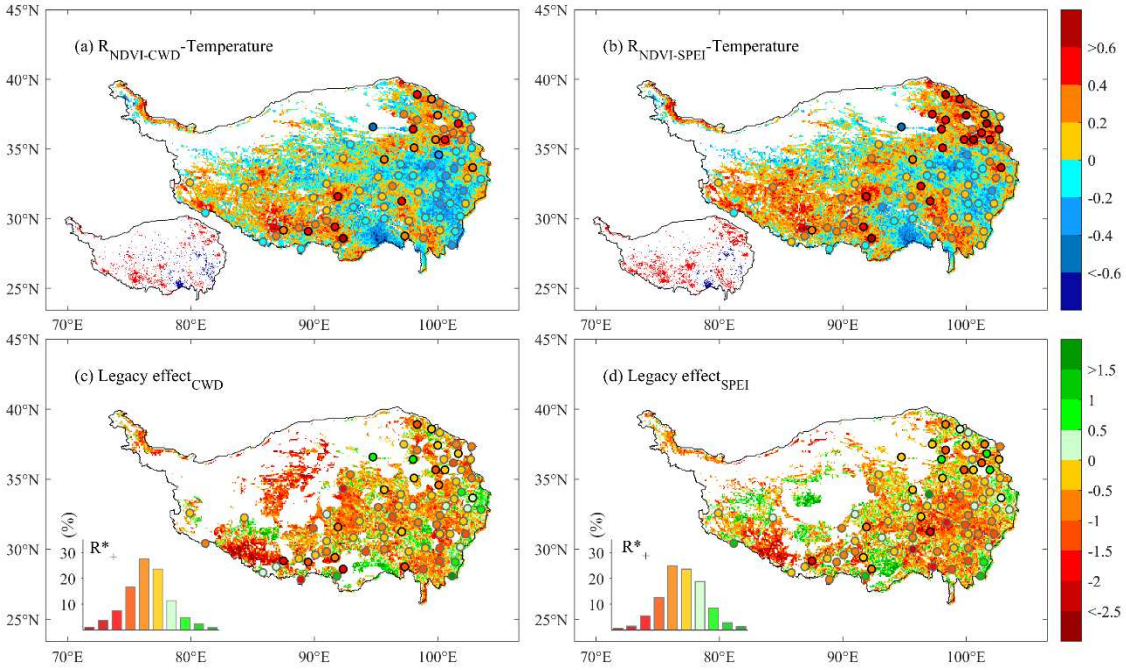

764

765 **Fig. A4.** Spatial patterns of partial correlation coefficients between growing season
766 NDVI and CWD (a), SPEI (b), and the legacy effects (after removing effects of
767 temperature by linear regression) in the first year post-drought derived from CWD (c),
768 SPEI (d). Colors of circles show results from meteorological sites (circles with black
769 edges represent sites with significant and positive correlation between NDVI and
770 CWD/SPEI, $p < 0.05$). Insets in (a) and (b) show the pixels with significant
771 NDVI-CWD/SPEI relationships (red: positive, blue: negative). Insets in (c) and (d)
772 show the frequency histograms of the legacy effects across pixels with significant
773 positive NDVI-CWD/SPEI relationships (R^*_+). Extra blank areas in (c) and (d) means
774 that no extreme drought event is detected during 1982-2015.

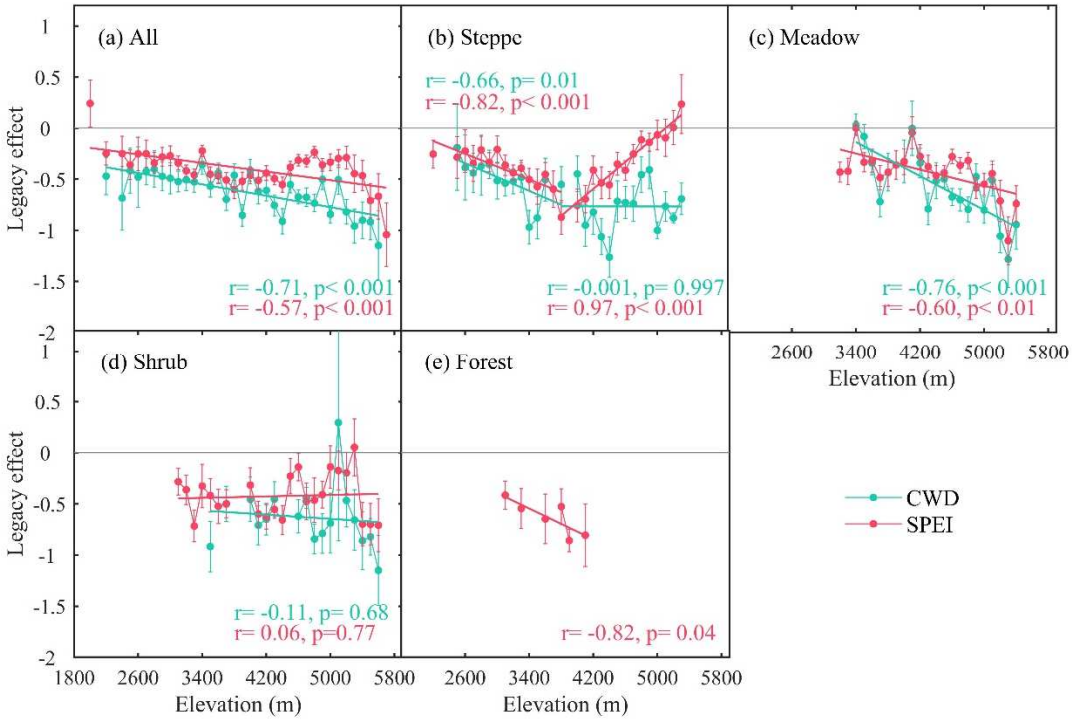

775

776 **Fig. A5.** Dependence upon elevation of legacy effect of NDVI (after removing effects
777 of temperature by linear regression) in the first year post-drought events derived from
778 SPEI and CWD. Only pixels with significant and positive correlation between NDVI
779 and SPEI/CWD and bins with at least 10 sample size were included in the analysis.
780 Error bars represent 95% confidence intervals around the mean from 1,000
781 bootstrapped estimates.

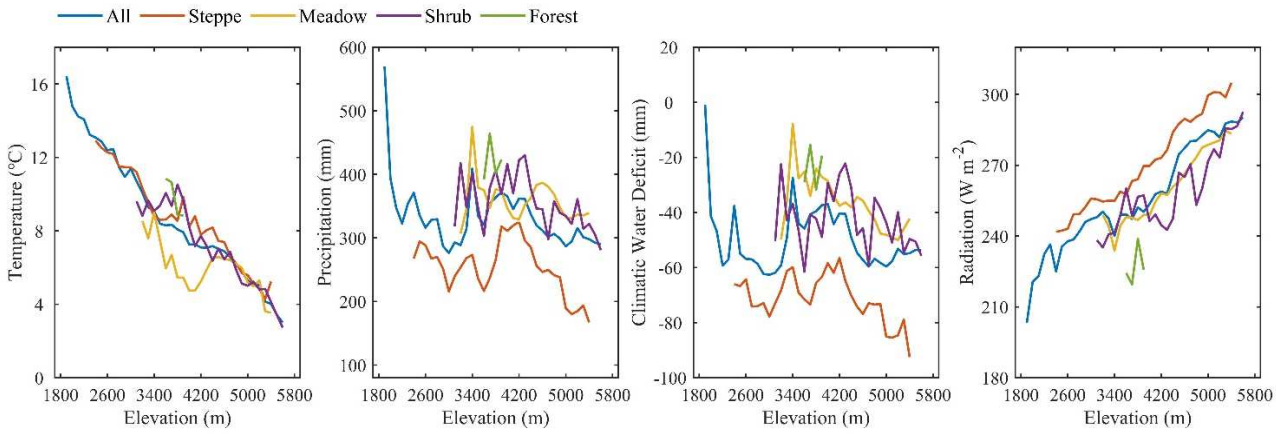

782

Fig. A6. Multi-year average growing season temperature, precipitation, climatic water deficit and downward shortwave radiation across the elevation gradients of the TP (at 100m interval bins). Only pixels with significant and positive correlation between NDVI and SPEI and bins with at least 10 sample size were included in the analysis.

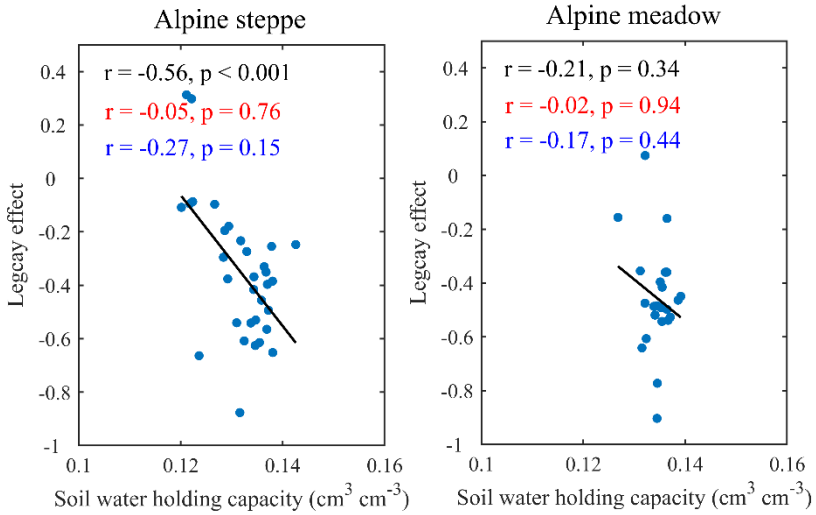

Fig. A7. Relationship between legacy effects on growing season NDVI in the first year post-drought and soil water holding capacity (WHC) in alpine steppe and meadow over the TP. Calculated linear correlation coefficient (black) and partial correlation coefficient controlling either CWD (red) or precipitation (blue) are also given with their significance levels. Dots represent average values within the 100m elevation bins. Only pixels with significant and positive NDVI-SPEI relationships were included in each elevation bin, and only bins with at least 10 sample size are shown here. WHC was calculated as field capacity minus permanent wilting point, which was from Dai et al. (2013), integrated over the top six layers of the dataset that correspond to the depth of 0~0.829 m.